

U-Pb Geochronology Zircon (LA-ICP-MS) data of the Gneissic-Migmatitic Complex of Salvador-Esplanada-Boquim Belt, São Francisco Craton, Brazil**Geocronologia U-Pb (LA-ICP-MS) em zircões do Complexo Gnáissico-Migmatítico do Cinturão Salvador-Esplanada-Boquim, Cráton do São Francisco, Brasil**

DOI:10.34117/bjdv6n10-577

Recebimento dos originais:08/09/2020

Aceitação para publicação:27/10/2020

Marcus Vinicius Costa Almeida Junior

Mestre em Geologia

Instituição: Universidade Federal do Recôncavo da Bahia (UFRB)

Endereço: Rua Rui Barbosa, 710, Centro, CEP 44.380-000. Cruz das Almas, Bahia, Brasil

E-mail: mvcajr@ufrb.edu.br

Angela Beatriz de Menezes Leal

Doutora em Geologia

Instituição: Universidade Federal da Bahia (UFBA)

Endereço: Rua Barão de Geremoabo, s/n, Campus Universitário de Ondina, CEP 40.170-290.

Salvador, Bahia, Brasil

E-mail: angelab@ufba.br

Johildo Salomão Figueirêdo Barbosa

Doutor em Geologia

Instituição: Universidade Federal da Bahia (UFBA)

Endereço: Rua Barão de Geremoabo, s/n, Campus Universitário de Ondina, CEP 40.170-290.

Salvador, Bahia, Brasil

E-mail: johildo.barbosa@gmail.com

Moacyr Moura Marinho

Doutor em Geologia

Instituição: Universidade Federal da Bahia (UFBA)

Endereço: Rua Barão de Geremoabo, s/n, Campus Universitário de Ondina, CEP 40.170-290.

Salvador, Bahia, Brasil

E-mail: mmm@ufba.br

ABSTRACT

The Salvador-Esplanada-Boquim Belt (SEBB) is considered a branch of the São Francisco Craton, located in its northeastern portion, in the Brazilian states of Bahia and Sergipe. This paper analyzed the U-Pb (LA-ICP-MS) geochronology on the Gneissic-Migmatitic Complex (GMC) zircons in the rocks of the SEBB. Six analyses were made on the rocks of GMC and two on granitic dykes. The obtained data allowed concluding that the GMC rocks were formed between $2150 \pm 19 - 2188 \pm 30$ Ma, while the dykes had their crystallization in line with the process of regional metamorphism in 2073 Ma. These metamorphic events are interpreted as products of the collision with the Serrinha

Block, provoking deformation, compression and uplifting of these rocks. After eroded, the granulitic roots of SEBB were exhumed, stabilizing on the way it is today with the GMC rocks, located on east and west of the Esplanada-Boquim Granulitic Complex.

Keywords: U-Pb Geochronology, LA-ICP-MS, Zircon, Salvador-Esplanada-Boquim Belt, São Francisco Craton.

RESUMO

O Cinturão Salvador-Esplanada-Boquim (CSEB) é considerado um ramo do Cráton do São Francisco, localizado na sua porção nordeste, nos estados brasileiros da Bahia e Sergipe. Neste trabalho foi analisada a geocronologia U-Pb (LA-ICP-MS) em zircões das rochas do Complexo Gnáissico-Migmatítico (CGM), pertencente ao CSEB. Foram realizadas seis análises nas rochas do CGM e duas em diques graníticos. Os dados obtidos permitiram concluir que as rochas do CGM se formaram entre $2150 \pm 19 - 2188 \pm 30$ Ma, enquanto que os diques tiveram a sua cristalização concomitante ao processo de metamorfismo regional, em 2073 Ma. Esses eventos metamórficos são interpretados como produtos da colisão com o Bloco Serrinha, gerando deformação, compressão e soerguimento dessas rochas. Posteriormente erodidas, exumou-se as raízes granulíticas do CSEB, estabilizando da forma como se encontra atualmente, com as rochas do CGM, situando-se a leste e oeste do Complexo Granulítico Esplanada-Boquim.

Palavras-chave: Geocronologia U-Pb, LA-ICP-MS, Zircão, Cinturão Salvador-Esplanada-Boquim, Cráton do São Francisco

1 INTRODUCTION

The importance of geochronological studies on metamorphic terrains derives from the possibility of accessing information from past conditions of our planet in different depths, pressure and temperature conditions for different types of rocks for both its lower crust and upper mantle, in other words, providing room for the analysis of the crust evolution throughout geological history, besides helping understand the chemical and tectonic processes referring to the crustal growth mechanics.

In Brazil, the São Francisco Craton (SFC) is considered one of the most complete registers of Precambrian geological events, consisting of Archean and Paleoproterozoic rocks, which include medium to high grade metamorphic rocks, remnants of greenstone belts, granites, syenites, mafic and ultramafic rocks (Barbosa and Sabaté, 2004). According to Hasui (2013), the SFC has an area that matches the Province of São Francisco, situated in center-east of Brazil, limited by the orogenic systems of Borborema to the north, Tocantins to the west, Mantiqueira and the Province of the Continental Margin to the east, and the Rio Preto Fold Belt to the northwest (Figure 1).

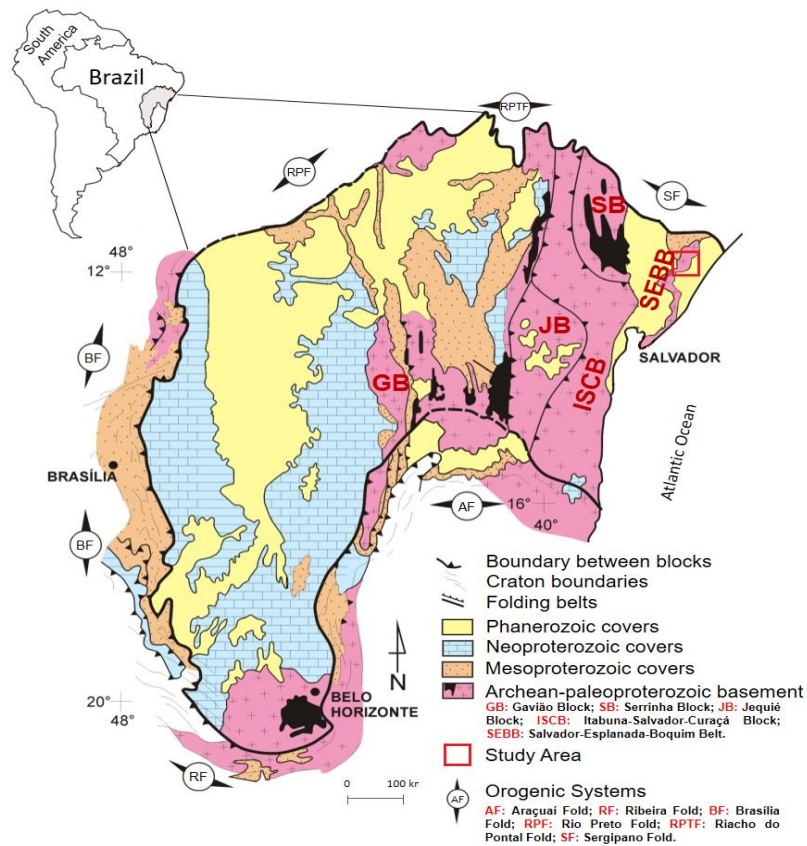
Tectonically, SFC is truncated by two rifts, being one of them guided by N-S direction and named Aulacogen of Paramirin by Pedrosa-Soares et al. (2001), having as characteristic units the Espinhaço (Paleoproterozoic) and São Francisco (Mesoproterozoic) Supergroups (Cruz and

Alkmin, 2007) and another one aged Mesozoic, on NNE-SSW direction that, according to Magnavita (1992), originated the Recôncavo-Tucano-Jatobá bay during the Gondwana fragmentation.

This Craton on the states of Bahia and Sergipe presents itself in four archean blocks, namely Gavião, Serrinha, Jequié and Itabuna-Salvador-Curaçá, besides the Salvador-Esplanada-Boquim Belt (SEBB) which, according to Barbosa and Sabaté (2002; 2004), collided in Paleoproterozoic, originating the Itabuna-Salvador-Curaçá Orogen (ISCO). It is in this orogen's most eastern portion that the rocks of the previously mentioned belt rise, which the study area of this work focuses on, more specifically on its gneissic-migmatitic rocks.

This work is therefore justified in accordance with the needs of understanding its tectonic and geochronological placing in the SFC regional context, adding new data and contributing to previously presented work by Almeida Junior et al. (submitted), related to petrographic and lithochemical aspects of these rocks and by Barbosa et al. (2018), who performed studies on the granulitic rocks that compose this belt. The focus of this work was hence obtaining geochronological data using the U-Pb method (Laser Ablation-ICP-MS) in zircons and the study area comprises the state of Sergipe southern portion and the state of Bahia northeastern portion.

Figure 1. Regional schematic sketch with the main SFC tectonic units, showing the study area.



Font: Modified from Alkmin et al., 1993.

2 GEOLOGICAL SETTING

The SFC development starts in the Archean period, with occurrences of new tectonomagmatic processes during the Paleoproterozoic (Teixeira and Canzian, 1994). The geological compartmentalization and the paleotectonic scenario according Teixeira (1992) can be observed through the individualization of exposed archean and proterozoic provinces both on the northerly and southerly portions being, in a general way, underlay by geological processes of volcanic, plutonic and sedimentary nature, besides metamorphic occurrences of medium and high degree.

In the states of Bahia and Sergipe, SFC subdivides into four blocks and a belt hereafter described in a synthetic way.

The Gavião Block is composed of orthogneiss tonalitic-granodioritic associations gneissic-amphibolite at times migmatized and metavolcanic sedimentary similar to greenstone belt sequences which possibly have their origin from the partial fusion of the ocean proto-crust, turning into one of the most ancient rocks of Latin American aging between 3.4 – 3.6 Ga, through the zircon U-Pb data (Bastos-Leal, 1998; Barbosa et al., 2012; Dantas et al., 1997; Oliveira et al., 2020).

The Serrinha Block is composed of gneisses and migmatites with subordinate amphibolites metamorphized on the amphibolite facies, all dating from the Archean, besides supracrustal metavolcanic sedimentary rocks aging from 3.0 to 3.3 Ga (Barbosa et al., 2012; Barbosa et al., 2018; Oliveira et al., 2011).

The Jequié Block, age Paleoproterozoic, consists of granulite-enderbite-trondhjemite, charnoenderbites and charnockites, as well as heterogeneous migmatized granulites and subordinate supracrustal rocks dating their prototypes from about 2.7 to 2.8 Ga. (Barbosa et al., 2001; 2012; Cordani, 1973).

The Itabuna-Salvador-Curaçá block basically consists of granulite-tonalite-trondhjemite and monzonitic to monzodioritic intrusions rebalanced on the granulite facies, besides the occurrence of supracrustal granulized rock enclaves and geographically spreads from the South of Bahia to the North edge of it (Barbosa et al., 2012).

Tectonically, the collage of these blocks took place in Paleoproterozoic at about 2.0 Ga, following a NW-SE compressional trend resulting on the formation of the Itabuna-Salvador-Curaçá Orogen, which throughout time and exhumation has suffered erosional processes, bringing to surface records of this ISCO's formation roots (Barbosa, 1990; Barbosa and Sabaté, 2002; Barbosa et al., 2012).

On the SFC eastern portion, in the states of Bahia and Sergipe, the rocks of Salvador-Esplanada-Boquim Belt emerge, aging from Archean-Paleoproterozoic, constituted by metamorphic rocks of medium and high degree apart from granitoids and associated mafic enclaves delimited by reverse faults and shear zones (Almeida Junior et al., submitted; Barbosa and Dominguez, 1996; Barbosa et al., 2018; Oliveira Júnior, 1990; Santos et al., 1997; Silva Filho et al., 1977).

The first group of metamorphic rocks studied by Santos et al. (1997), Melo de Oliveira (2014) and Barbosa et al. (2018) is called Esplanada-Boquim Granulitic Complex, formed by orthogneiss charnoenderbites to charnockites, kinzigites gneisses, calc-silicatic rocks, metanorites and biotites migmatized gneisses from acid to intermediate nature, besides subordinate quartzite lenses with crystallization ages in 2582 ± 11 Ma and regional metamorphism event between 2087 and 2073 Ma. According to Santos et al. (1997), this complex is limited on east and west by the Gneissic-Migmatitic Complex (GMC) and on north by the rocks of Estância Group and detritus covers of Barriers Group.

The Gneissic-Migmatitic Complex (GMC), studied by Almeida Junior et al. (submitted), is formed by an orthogneissic acid-basic association of amphibolitic nature with granitic and granodioritic protoliths, with occurrences of varied degrees of migmatization, intruded by late granitoids and punctual granulitic intercalations. This Migmatitic Complex takes place on the southly portion of the SEBB subdivided in two stripes diverging away to the north, separated by the Esplanada-Boquim Granulitic Complex.

There is still the occurrence of a dyke swarm of an acid-intermediate nature with subordinate basic terms that truncate the Gneissic-Migmatitic and Granulitic Complex rocks between the cities of Arauá and the municipality of Tanque Novo on the state of Sergipe, constituted of rhyolite and porphyritic dacite (Santos et al., 1997).

3 ANALYTIC METHODS

This paper restrains to the geochronological study of GMC aiming to complement the field, petrographic and lithochemical works performed by Almeida Junior et al. (submitted) and contribute to the understanding of the Salvador-Esplanada-Boquim Belt, gathering the information obtained from Melo de Oliveira (2014) and Barbosa et al. (2018) about Esplanada-Boquim Granulitic Complex.

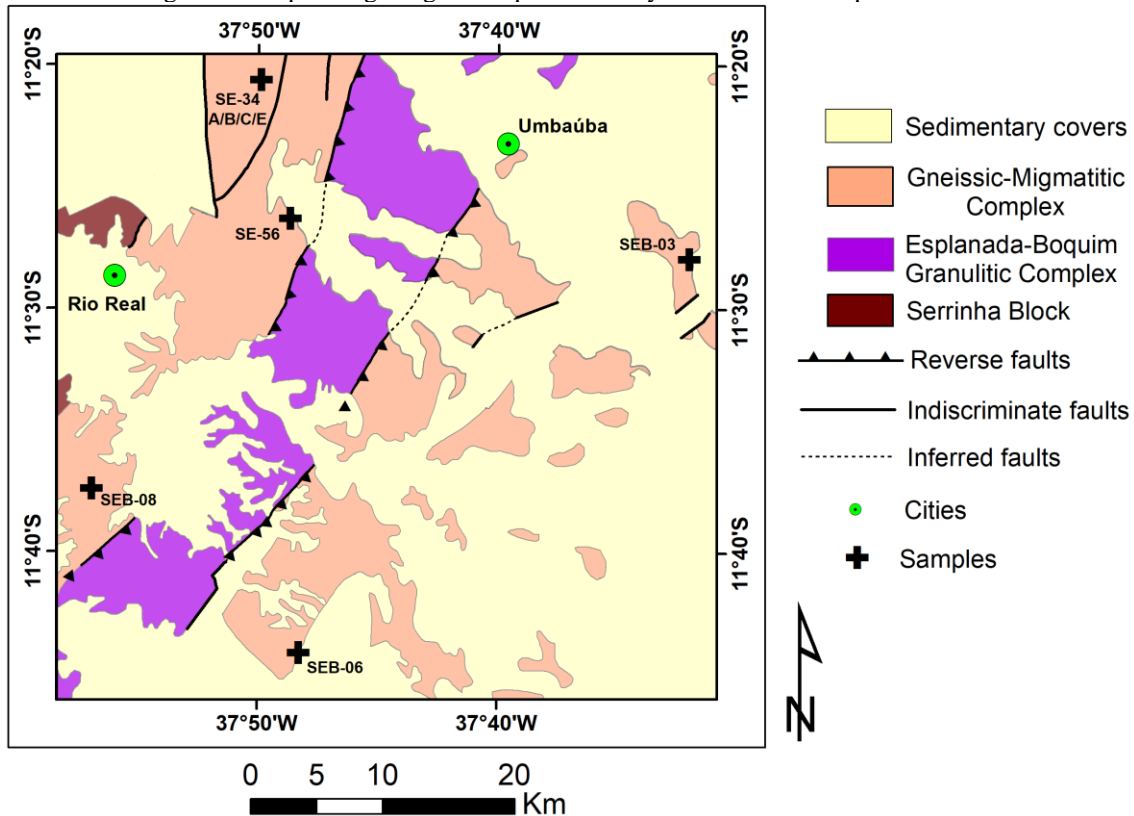
Figure 2 shows the simplified geologic map of the studied region highlighting the samples location used for the U-Pb zircon dating (LA-ICP-MS). Following, the outcrops and the collected samples will be described.

The samples SE-34A, SE-34B, SE-34C, SE-34E and SE-56 were analyzed by the Ouro Preto Federal University (UFOP) Geosciences Department and the samples SEB-03, SEB-06 and SEB-08 in the High Resolution Laboratory of the São Paulo University's Geosciences Institute (IGc-USP).

The samples were submitted to scrutiny following the Laser Ablation-ICP-MS method, using a Q-ICP-MS Angilent 7700 piece of equipment and a New Wave 213 nm laser. The standards and the sample case were washed in acid before the analyses in order to remove possible Pb contaminations on their surfaces. The relevant isotopic ratios ($^{207}\text{Pb}/^{206}\text{Pb}$, $^{208}\text{Pb}/^{206}\text{Pb}$, $^{208}\text{Pb}/^{232}\text{Th}$, $^{206}\text{Pb}/^{238}\text{U}$ and $^{207}\text{Pb}/^{235}\text{U}$, in which ^{235}U was calculated from ^{238}U through the natural abundance of the ratio $^{235}\text{U} = ^{238}\text{U} / 137.88$) were calculated using the reduction data from Glitter software (Van Achterbergh et al., 2001). International patterns such as 609 MaGemoc (Jackson et al., 2004) and 337 MaPlessovice (Sláma et al., 2008) were used. Yet, the use of photomicrography was done over the light that was transmitted and reflected together with cathode-luminescence (CL) imaging, using micro-sound electronic scanning (MES) so as to assess details about the zircon crystals growth.

The ages were stamped on the concordia diagram using the isoplot v. 2.2 (Ludwig, 2001) software, moreover all uncertainties of individual analyses are about 1σ and all analyses on the calculi of concordant and intercepting ages are about 2σ .

Figure 2. Simplified geological map of the study area with the samples locations



Font: Modified from GEOTERM, 2010.

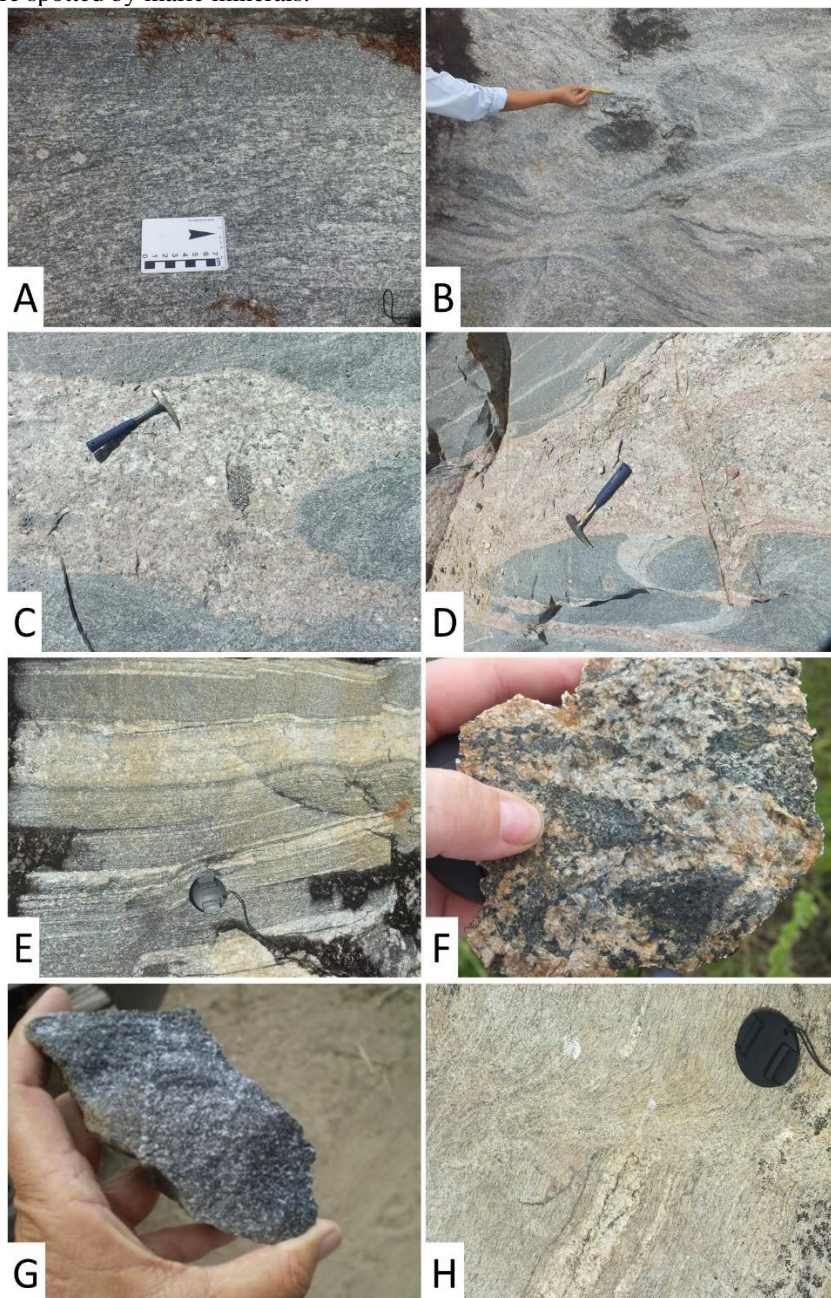
4 SAMPLING

From the petrographic and lithochemical studies Almeida Junior et al. (submitted) suggests that the Gneissic Migmatitic Complex is of granitic and granodioritic nature, chemically formed by sodic, intermediate and potassic groups placed between these two extremes. Tectonically, the rocks of this complex were classified as being from a syn collisional to volcanic arch environment, the same environment proposed by Barbosa et al. (2018) for the Esplanada-Boquim Granulitic Complex.

The sample SE-34A is the dark-grey portion referring to the paleossoma and is mesoscopically classified as a gray orthogneiss (Figure 3A); the sample SE-34B refers to the leucosome in light gray color, presenting itself, macroscopically, as a gneissic granodiorite (Figure 3B); the sample SE-34C is a leucogranitic dyke with fine discontinuous biotite segregations amidst the saccharoidal aggregate of rosy white segregates (Figure 3C); the sample SE-34E is a massive rosy granitic dyke constituted of an equigranular rosy, white and quartz and feldspar aggregate with disseminate biotite reeds (Figure 3D); the sample SE-56 corresponds to a rock flooring consisting of a well-foliated banded biotite orthogneiss of medium granulation, equigranular and tonalitic to granodioritic composition (Figure 3E); the sample SEB-03 constitutes a banded orthogneiss, well-foliated with thin to medium granulation and bands in quartz feldspar creamy color and dark

greenish bands with a greater proportion of mafic minerals (Figure 3F); the sample SEB-06 is a dark thin amphibolite with extremely thin white plagioclase crystals amidst prismatic oriented hornblende crystals (Figure 3G) and the sample SEB-08 consists of a massive black and white-spotted granitoid, formed by granulate to tabular crystals disposed randomly of white and lightly rosy feldspars with thin quartz in the interstitials (Figure 3H).

Figure 3. Macroscopic aspects of the samples. A) Orthogneiss general view on its gray paleossomatic portion of the GMC. B) View of the leucossomatic portion of the GMC outcrop in light gray. C) General view of the leucossomatic granite dyke intruding the GMC rocks. D) Macroscopic view of the rosy granitic dyke in contact with the gneiss migmatitic orthogneiss. E) Outcrop view highlighting the orthogneiss compositional banding in this unit. F) Orthogneiss macroscopic sample highlighting the creamy color portions of quartz feldspar and the dark greenish mafic mineral ones. G) Macroscopic sample highlighting the rock's amphibolitic characteristic. H) Granitoid's outcrop view highlighting its leucocratic feature spotted by mafic minerals.



5 RESULTS AND DISCUSSION

The data from the eight geochronological analyses are listed on Table 1 and are described separately below.

5.1 SAMPLE SE-34A

Zircons extracted from this sample are dominantly prismatic ranging from 30 μm to 300 μm long. Most grains preserve long prismatic shapes, but many are invariably broken into half and show with round terminations. Optically the grains are brown and dark brown - many of which are translucent to partly translucent. Cathode-luminescence (CL) images reveal poorly developed zoning. The grains are rather marked by structureless patchy interiors with bright and dark domains. A limited number of grains shows core-rim relationships. In this case, structureless/irregular cores are surrounded by thin CL-bright or CL-dark rims.

LA-ICP-MS spots on the irregular cores gave substantially old apparent $^{206}\text{Pb}/^{207}\text{Pb}$ ages (2600 – 2850 Ma), but most points are highly discordant and thus no age reduction was attempted. Analyses on the structureless grains, with both dark and bright domains, gave points that are discordant to slightly concordant on the concordia diagram. The most concordant points align along a recent, Pb-loss discordia line that intercepts the upper concordia at 2159 ± 11 Ma (MSWD = 3). This age is similar (within error) to a concordant age of 2166 ± 13 Ma, which is given by six concordant points. Therefore, the concordant age is interpreted as being the rock's crystallization age and consequently the orthogneiss formation (Figure 4A).

5.2 SAMPLE SE-34B

Zircons extracted from this sample range from 30 to 300 μm long, and preserve short and long prismatic shapes. Most grain record round terminations are invariably metamict and inclusion-rich. They vary in color from dark brown to slight translucent brown. They also record complex internal zoning under the CL detector, with very poorly defined core-rim structures. Large prismatic grains seem to record structureless rims that surround CL bright cores. Analyses on the centre of several prismatic structureless grains gave points that are discordant on the concordia diagram.

A close inspection of the data for individual spots shows that the Pb analyses were affected by inclusions of apatite and titanite. No age was attempted because of discordance and high Pb^{204} content. Analyses on partly translucent rims of a few prismatic grains gave five concordant to subconcordant points that seem to define one population. The points align along a discordia line that intercepts the upper concordia at 2080 ± 49 Ma. A similar, but more precise age is given by three

concordant points that give a concordia age of 2073 ± 12 Ma (MSWD = 0.9), interpreted as referring to the dyke crystallization associated with the GMC regional metamorphism (Figure 4B).

5.3 SAMPLE SE-34C

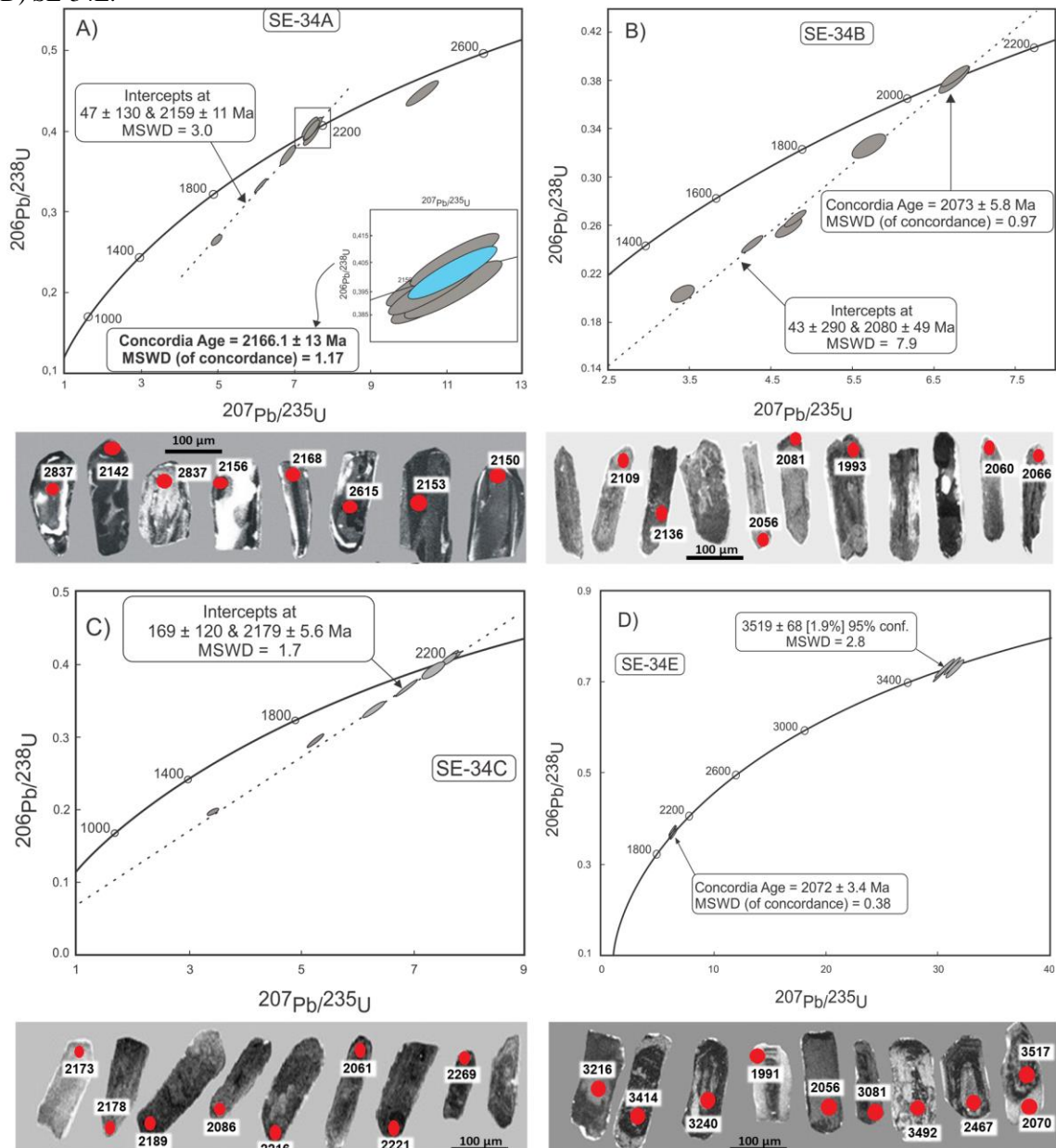
This sample shows zircons that preserve long prismatic shapes with sharp and round terminations respectively. All grains range in color from dark brown to slight translucent brown. Most grains are marked by low luminescence under the CL detector. No core-rim relationship was clearly observed. Analyses on the centre and edges of several prismatic grains gave points that are highly discordant on the concordia diagram. A number of round structureless grains gave highly discordant points with $^{206}\text{Pb}/^{207}\text{Pb}$ apparent ages ranging from 2700 to 3400 Ma. Nevertheless, five partly translucent grains gave concordant to subconcordant points, which seem to define one population. These points align along a discordia line that intercepts the upper concordia at 2179 ± 6 Ma (MSWD = 1.7), interpreting the age of this rock's formation similarly to the one shown in SE-34A (Figure 4C).

5.4 SAMPLE SE-34E

Zircons extracted range from small to large (30-300 μm), and preserve short to long prismatic shapes with sharp and round terminations respectively. All grains are inclusion rich, partly metamict and range in color from dark brown to slight translucent brown. Small grains are partly translucent and were less affected by metamictization. The long prismatic grains record complex structures under the CL detector. Small grains (30-80 μm) have poorly developed zoning and may show dark cores enveloped by brighter rims. Analyses on the core of several prismatic grains gave points that are highly discordant on the concordia diagram.

Four concordant to reversely discordant grains give an age of 3519 ± 68 Ma (MSWD=2.8). However, this age should be interpreted with care as the points may not represent one single population. Further attempts to obtain more precise ages of the dataset have failed, given the highly heterogeneous nature of the individual grains. The analyses were largely compromised by the size of the grains, but overall six of these points seem to define a population with a concordia age of 2072 ± 7 Ma (MSWD = 0.38), referring to the crystallization of this rock, concomitantly to the GMC metamorphism event (Figure 4D).

Figure 4. Concordia diagrams and zircon grain images from cathode luminescence. A) SE-34A, B) SE-34B, C) SE-34D, D) SE-34E.



5.5 SAMPLE SE-56

The images from CL show well-zoned prismatic zircons, some of them having shown very distinct bright cores. Some of these cores can present magmatic corroded features. Most grains, however, do not present such evident cores but a strong chemical zoning, typical of crystallization from magma. This is consistent with the homogeneity of the analyses obtained from LA-ICP-MS. Some analyses in well-zoned zircons granted concordant and subconcordant points of average $^{207}\text{Pb}/^{206}\text{Pb}$ of 2151 ± 13 Ma. A more accurate age of 2151.1 ± 6.9 Ma is given by the discordia line that passes by all points obtained for this sample. This age is seen as the orthogneiss crystallization

and formation age. All bright cores' ages were analyzed and belong to the same group which gives in average the value of 2150 Ma (Figure 5A).

5.6 SAMPLE SEB-03

The zircon grains from this sample are euhedric and subeuhedric varying in size from 100 μm to 400 μm in length and presenting an approximate 2:1 ratio between length and height. In a general way, the CL images show prismatic habit and the presence of zoning. The contact between core and the zircon growth halos is rounded presenting different levels of zoning. The analyses align over discordia, with ages varying from 1086 ± 14 Ma a 2484 ± 31 Ma, intercepting concordia on the lower part in 741 ± 110 Ma and on the upper in 2518 ± 32 Ma (MSWD = 5.4). Although one sample coincided with concordia also presenting 2188 ± 30 Ma. These data are interpreted as coming from the crystallization of the rock and consequent orthogneiss formation (Figure 5B).

5.7 SAMPLE SEB-06

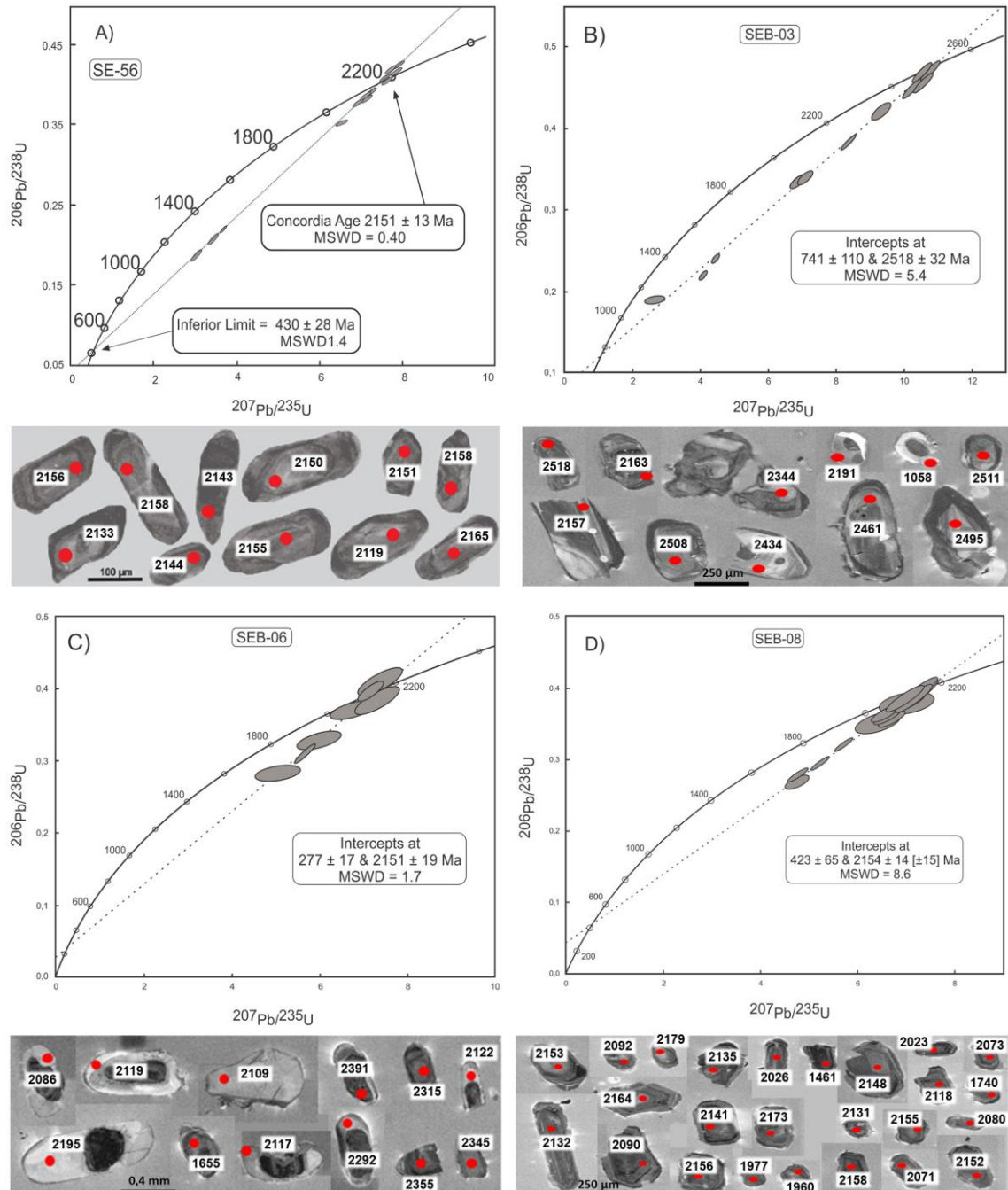
The zircons from Sample SEB-06 are rounded (anedric) and the zonings present great distinction, varying approximately from 0.2 to 1 mm in size. Some zircons have fractures either on the core or on the rims, presenting low intensity cathode luminescence around the cores, but with higher intensity near the rims. The images from the cores and rims are plotted on the concordia diagram and show concentration around the discordia line when higher than 150 Ma, with six more concordant points intercepting concordia in 2150 ± 19 Ma (MSWD = 1.7), referring to the environment of the orthogneisses formation. Other three samples present older concordant ages comparing to the previous population, varying from 2229 ± 41 Ma a 2383 ± 33 Ma, being it possibly related to the reliquary zircons from the Esplanada-Boquim Granulitic Complex granulitization (Figure 5C).

5.8 SAMPLES SEB-008I AND SEB-08II

The samples SEB-08I and SEB-08II refer to the point and despite the zircons morphological description had been done separately, the geochronological analysis was plotted on a single concordia diagram. The zircons from sample SEB-08I vary from 100 to 200 μm , predominantly prismatic with some rounded borders, well defined growth zoning and low intensity of cathode luminescence in the cores and moderate on the rims. The ones referring to sample SEB-08II vary from 0.2 to 1 mm, predominantly subhedral with rounded rims, stretched grains and apparent zoning in part of the sampling population, besides there is low intensity of CL both on the cores and on the rims. The Concordia diagram shows two population agglomerations plotting the discordia line, the

first varying from approximately 1400 to 1800 Ma and the second with 12 samples already intercepting Concordia in 2154 ± 14 Ma (MSWD = 8.6), whose analyses allow interpreting this age as the rock's crystallization (Figure 5D).

Figure 5. Concordia diagrams and zircon grains cathode luminescence images. A) SE-56; B) SEB-03, C) SEB-06, D) SEB-08.



6 CONCLUSION

The geochronological data from this work allowed concluding that the orthogneiss rocks which belong to the GMC formed in a period between 2150 ± 19 and 2188 ± 30 Ma after the

Salvador-Esplanada-Boquim Belt granulitic rock formation studied by Barbosa et al. (2018), taking place between 2473 ± 13 and 2582 ± 11 Ma.

The leucogranitic dykes obtained ages (sample SE-34C) and the rosy one (sample SE-34E) were of 2073 ± 12 Ma and 2072 ± 07 Ma respectively, they coincide with the age proposed by Melo de Oliveira (2014) as being driven from the main metamorphic regional event of the Salvador-Esplanada-Boquim Belt, suggesting the crystallization of these dykes is related to this metamorphism.

Therefore, the joint interpretation of both the data found in this research and the ones from Melo de Oliveira (2014) and Barbosa et al. (2018) allow inferring that the rocks from the Esplanada-Boquim Granulitic Complex were formed during the Siderian period and followed by the orthogneissic rocks crystallization of the Gneissic Migmatitic Complex during the Rhyacian period. All these groups were then exposed to the regional metamorphism event by the end of the Rhyacian period (2073 ± 12 Ma and 2072 ± 07 Ma), allowing the intrusion and then crystallization of the predominantly granitic dykes.

These metamorphic events are interpreted as derived from the collisions with the Serrinha Block, stabilized between 3.1 – 2.8 Ga (Barbosa et al., 2012), causing deformation and compression on the Salvador-Esplanada-Boquim Belt with reverse faults and shear zones mapped by Santos et al. (1997) and Melo de Oliveira (2014). These compressive events originated the chain of mountains that were later eroded allowing the exhumation of the SEBC granulitic roots on this research, placed to the east and west of the Esplanada-Boquim Granulitic complex, as shown in Figure 2.

REFERENCES

- Alkmim, F.F., Brito Neves B.D., Alves, J.C., 1993. Arcabouço tectônico do Cráton do São Francisco-uma revisão. In: Dominguez, J. M. L., Misi, A. (Eds.). O Cráton do São Francisco. SBG-Núcleo BA/SE, 1: 45-62.
- Almeida Junior, M.V.C., Menezes Leal, A.B., Barbosa, J.S.F., Marinho, M.M., submitted. As raízes gnáissico-migmatíticas do Cinturão-Salvador-Esplanada-Boquim, Cráton do São Francisco, Brasil.
- Barbosa, J.S.F., 1990. The granulites of the Jequié complex and Atlantic mobile belt, southern Bahia, Brazil: an expression of Archean-Proterozoic plate convergence. In: D. Vielzeuf, P. Vidal (Eds.), *Granulites and Crustal Evolution*, 195-221. France: Springer-Verlag.
- Barbosa, J.S.F., Dominguez, J.M.L., 1996. Texto Explicativo para o Mapa Geológico ao Milionésimo da Bahia. Salvador, SICM/SGM, 400 p.
- Barbosa, J.S.F., Sabaté, P., 2002. Geological features and the Paleoproterozoic collision of four Archaean Crustal segments of the São Francisco Craton, Bahia, Brazil. A synthesis. *Anais da Academia Brasileira Ciências*, 74(2), 343-359. <http://dx.doi.org/10.1590/S0001-37652002000200009>
- Barbosa, J.S.F., Sabaté, P., 2004. Archean and Paleoproterozoic crust of the São Francisco Craton, Bahia, Brazil: geodynamic features. *Precambrian Research*, 133:1-27. <http://dx.doi.org/10.1016/j.precamres.2004.03.001>
- Barbosa, J.S.F., Correa Gomes, L.C., Marinho, M.M., Silva, F.C.A., 2001. Geologia do segmento sul do Orógeno Itabuna-Salvador-Curaçá. I Workshop sobre o Orógeno Itabuna-Salvador-Curaçá. Salvador, Bahia.
- Barbosa, J.S.F., Cruz, S.P., Souza, J.S., 2012. Terrenos Metamórficos do Embasamento, In: Barbosa, J. S. F. (ed.) *Geologia da Bahia: pesquisa e atualização*. Série Publicações Especiais, 13 Convênio CBPM/UFBA-IGEO/SBG. 2v.
- Barbosa, J.S.F., Marinho, M.M., Menezes Leal, A. B., Oliveira, E.M., Souza-Oliveira, J.S., Argollo, R.M., Lana, C., Barbosa, R.G., Santos, L.T.L., 2018. As raízes granulíticas do Cinturão Salvador-Esplanada-Boquim, Cráton do São Francisco, Bahia-Sergipe, Brasil. *Geologia USP, Série Científica*, 18(2): 103-128. <https://doi.org/10.11606/issn.2316-9095.v18-134238>
- Bastos-Leal, L.R., 1998. Geocronologia U/Pb (Shrimp), Pb/Pb, Rb-Sr, Sm-Nd e K-Ar dos Terrenos granito-Greenstone do Bloco Gavião: Implicações para a Evolução arqueana e proterozoica do cráton do São Francisco, Brasil. São Paulo, 178p. Tese de Doutorado, Programa de Pós-Graduação em Geoquímica e Geotectônica, Instituto de Geociências, Universidade do Estado de São Paulo.
- Cordani, U.G., 1973. Evolução geológica pré-Cambriana da faixa costeira do Brasil entre Salvador e Vitória. Tese de Doutorado, Instituto de Geociências, Universidade de São Paulo, 98p. São Paulo.
- Cruz, S.C.P., Alkmim, F.F., 2007. A história de inversão do aulacógeno do Paramirim contada pela sinclinal de Ituaçu, extremo sul da Chapada Diamantina (BA). *Revista Brasileira de Geociências*, 37(4): 92-110.

Dantas, E.L., Brito Neves, B.B., Fuck, R.A., 2010. Looking for the oldest rocks of South America: Paleoproterozoic orthogneiss of the Sobradinho Block, northernmost foreland of the São Francisco Craton, Petrolina, Pernambuco, Brazil. VII South American Symposium on Isotope Geology (SSAGI), Brasilia, pp. 137–140. S0136.

GEOTERM-NE, 2010. Geração de calor nas bacias de Cumuruxatiba, Jequitinhonha, Sergipe-Alagoas e Pernambuco-Paraíba, e nos embasamentos a elas adjacentes. Patrocinado pelo Promob-Cenpes-Petrobras e executado pelo CPGG-UFBA.

Hasui, Y., 2013. Cráton São Francisco, In: Almeida, F.F.M., Bartorelli, A., Carneiro, F.D.R., Hasui, Y., (Eds.) Geologia do Brasil. Ed. Beca, São Paulo, 900p.

Jackson, S.E., Pearson, N.J., Griffin, W.L., Belouso-Va, E.A., 2004. The application of laser ablation inductively coupled plasma mass spectrometry to in situ U-Pb zircon geochronology. *Chem Geol* 211: 47–69.

Ludwig, K.R., 2001. Isoplot/Ex, rev. 2.49. A Geochronological Toolkit for Microsoft Excel. Berkeley Geochronology Center, Special Publication n°. 1a.

Magnavita, L.P., 1992. Sistema de borda de rift: inter-relação entre tectonismo e sedimentação do rift do Recôncavo-Tucano-Jatobá, NE Brasil. In: XXXVII Congresso Brasileiro de Geologia, São Paulo, SBG. Anais, p.567-568.

Marinho, M.M., 1991. La séquence vulcano-sédimentaire de Contendas-Mirante et La Bordure Occidentale Du Bloc Jequié (Craton Du S. Francisco-Bresil): Um exemple du transition Archéean-Protérozoïque. Tese (Doutorado). Clermont Ferrand: Blaise Pascal University, 388p.

Martin, H., Sabaté, P., 1990. Características geoquímicas do Maciço de Sete Voltas no Cinturão Contendas-Mirante (Bahia): implicações na evolução petrogenética de um segmento arqueano do Cráton do São Francisco. XXXVI Congresso Brasileiro de Geologia, Resumos. Natal: SBG.

Martin, L., Suguio, K., Dominguez J.M.L., 1997. Geologia do Quaternário Costeiro do litoral Norte do Rio de Janeiro e do Espírito Santo, CPRM, Belo Horizonte, 125p.

Melo de Oliveira, E., 2014. Petrografia, litogeoquímica e geocronologia das rochas granulíticas da parte norte do Cinturão Salvador-Esplanada-Boquim, Bahia-Sergipe. Tese de Doutorado, Programa de Pós Graduação em Geologia, Instituto de Geociências, Universidade Federal da Bahia, 220p.

Oliveira, E.P., Souza, Z.S., McNaughton, N.J., Lafon, J.M., Costa, F.G., Figueiredo, A.M., 2011. The Rio Capim volcanic–plutonic–sedimentary belt, São Francisco Craton, Brazil: Geological, geochemical and isotopic evidence for oceanic arc accretion during Palaeoproterozoic continental collision. *Gondwana Research*, 19(3): 735-750.

Oliveira, E.P., McNaughton, N.J., Zincone, S.A., Talavera, C., 2020. Birthplace of the São Francisco Craton, Brazil: Evidence from 3.60 to 3.64 Ga Gneisses of the Mairi Gneiss Complex. *Terra Nova*, 00:1–9. <https://doi.org/10.1111/ter.12460>.

Oliveira Junior, T.R., 1990. Geologia do extremo nordeste do Cráton do São Francisco. Dissertação (Mestrado). Salvador: Instituto de Geociências – UFBA, 102p.

Pedrosa-Soares, A.C., Noce, C.M., Wiedmann, C.M., Pinto, C.P., 2001. The Araçuaí-West-Congo Orogen in Brazil: an overview of a confined orogen formed during Gondwanaland assembly. *Precambrian Research*, 110(1/4) p. 307-323.

Santos, R.A., Martins, A.A.M., NEVES, J.P., LEAL, R.A., 1997. Geologia e Recursos Minerais do Estado de Sergipe. Texto Explicativo do Mapa Geológico de Sergipe. Brasília: CPRM; Sergipe: CODISE, 156p.

Silva Filho, M.A., Bomfim, L.F.C., Santos, R.A., Santana, A.C., Braz Filho, P.A., 1977. Projeto Baixo São Francisco/Vaza-Barris: Folha Cipó, Escala 1:250.000, Estado da Bahia. Programa Levantamentos Geológicos Básicos do Brasil. Convênio DNPM/CPRM, Brasília: CPRM, 187p.

Sláma, J., Kosler, J., Condon, D.J., Crowley, J.L., Gerdes, A., Hanchar, J.M., Horstwood, M.S.A., Morris, G.A., Nasdala, L., Norberg, N., Schaltegger, U., Schoene, B., Tubrett, M.N., Whitehouse, M.J., 2008. Plesovice zircon – A new natural reference material for U–Pb and Hf isotopic microanalysis. *Chemical Geology*, 249(1–2), 1–35.

Teixeira, W., 1992. Contribuição ao conhecimento geocronológico do Cráton do São Francisco: avaliação de dados isotópicos em rochas ígneas e metamórficas - implicações na evolução crustal pré-cambriana. Tese de Livre-Docência. Instituto de Geociências, Universidade de São Paulo, 172p.

Teixeira, W., Canzian, F., 1994. A evolução tectonotermal proterozoica do Cráton do São Francisco, com base em interpretações geocronológicas K-Ar em rochas do seu embasamento. *Bol. IG-USP, Série Científica*, 25:61-80.

Van Achterbergh, E., Ryan, C.G., Jackson, S.E., Griffin, W.L., 2001. Data reduction software for LA–ICP–MS, in Sylvester P.J. (ed.), *Laser ablation–ICP–mass spectrometry in the Earth Sciences: Principles and applications*. Ottawa, Ontario, Mineralogical Association of Canada, Short Course Series, 29, 239–243.